

PARALLEL CPU-GPU EXECUTION FOR LLM INFERENCE ON CONSTRAINED GPUS

Jiakun Fan, Yanglin Zhang, Xiangchen Li, Dimitrios S. Nikolopoulos

ABSTRACT

Deploying large language models (LLMs) for online inference is often constrained by limited GPU memory, particularly due to the growing KV cache during auto-regressive decoding. Hybrid GPU-CPU execution has emerged as a promising solution by offloading KV cache management and parts of attention computation to the CPU. However, a key bottleneck remains: existing schedulers fail to effectively overlap CPU-offloaded tasks with GPU execution during the latency-critical, bandwidth-bound decode phase. This particularly penalizes real-time, decode-heavy applications (e.g., chat, Chain-of-Thought reasoning) which are currently underserved by existing systems, especially under memory pressure typical of edge or low-cost deployments.

We present APEX, a novel, profiling-informed scheduling strategy that maximizes CPU-GPU parallelism during hybrid LLM inference. Unlike systems relying on static rules or purely heuristic approaches, APEX dynamically dispatches compute across heterogeneous resources by predicting execution times of CPU and GPU subtasks to maximize overlap while avoiding scheduling overheads. Critically, APEX is the first system to achieve fine-grained runtime CPU offloading without resorting to batch splitting, a common compromise that can hinder performance in prior hybrid systems. APEX targets common workload patterns in multi-turn conversation and reasoning tasks, where prefill stages are brief but decode phases are long and performance-critical.

We evaluate APEX on diverse workloads and GPU architectures (NVIDIA T4, A10), using LLaMa-2-7B and LLaMa-3.1-8B models. Compared to GPU-only schedulers like VLLM, APEX improves throughput by 84%–96% on T4 and 11%–89% on A10 GPUs, while preserving latency. Against the best existing hybrid schedulers, it delivers up to 49% (T4) and 37% (A10) higher throughput in long-output settings. APEX significantly advances hybrid LLM inference efficiency on such memory-constrained hardware and provides a blueprint for scheduling in heterogeneous AI systems, filling a critical gap for efficient real-time LLM applications.

1 INTRODUCTION

The increasing scale and capabilities of Large Language Models (LLMs) [4, 29, 36, 30, 12] have led to significant advancements across diverse applications. However, deploying these models, particularly state-of-the-art variants, imposes substantial demands on the underlying hardware infrastructure. Furthermore, eliciting sophisticated reasoning through techniques like Chain-of-Thought [31, 19] necessitates the generation of extended output sequences. While GPUs provide the high computational throughput essential for LLMs, generating these extended sequences via auto-regressive decoding involves numerous steps. Although the computational work per decode step is typically less intensive than the highly parallel prefill stage, the cumulative computation across many tokens becomes substantial. More critically for system constraints, this iterative process leads to the generation of a large and growing KV cache for the attention mechanism. This KV cache increases linearly with sequence length, and its storage becomes a primary concern [13, 20, 24].

The limited and costly onboard memory (VRAM) of these GPUs then presents a critical system bottleneck for accommodating this cache. LLM engines store this KV cache in GPU memory to reuse previous computations in the self-attention layer, and its substantial memory footprint limits the batch size. Even though parameter sharing across multiple batched requests can effectively increase arithmetic intensity for linear operation layers (like Q, K, V, O projections and feed-forward networks), the KV cache memory often becomes the limiting factor for achieving optimal GPU utilization and throughput, especially on

memory-constrained devices. Consequently, equipping servers with sufficient high-capacity GPUs to host large models and their growing KV caches incurs prohibitive costs, and maximizing hardware utilization through request batching further intensifies this GPU memory pressure [20].

This tension between growing KV cache memory demands and limited GPU memory creates a compelling opportunity to rethink the division of labor between CPUs and GPUs during LLM inference. Modern servers can readily be configured with terabytes of DRAM, motivating hybrid CPU-GPU inference systems. Prior work has explored various solutions, including quantization [35, 21, 15] to reduce memory consumption, albeit sometimes at the cost of accuracy. Another significant line of work involves offloading model weights, the KV cache, or even computation to the CPU [20, 26, 38, 27, 33, 34]. Initial memory offloading approaches focused on less frequently accessed data, like model parameters or parts of the KV cache, transferring them back when needed [20, 26]. However, the KV cache is accessed at every decoding step, making frequent data transfers over the relatively slow CPU-GPU interconnect (e.g., PCIe) a significant performance bottleneck, rendering many such techniques that rely on layer-by-layer swapping unsuitable for latency-sensitive online inference [13, 26].

Recognizing this challenge, more recent research [13, 16] proposes a more fundamental shift: decomposing the transformer’s phase and executing the inherently memory-bound attention computations (involving KV cache access) directly on CPUs, leveraging their attached high-capacity DRAM. While compute-intensive parts like MLP layers remain on the GPU, this partitioning allows the CPU to act as an active compute participant for memory-heavy tasks, performing them “near-memory” without repetitive, costly GPU transfers.

Crucially, this insight holds the promise of freeing substantial GPU memory, enabling larger batch sizes, improving GPU utilization, and boosting overall throughput, especially when GPU memory is constrained. However, translating this concept into practical, efficient systems presents significant hurdles. Achieving optimal performance with CPU-offloaded attention requires careful management of heterogeneous resources and precise scheduling to maximize parallelism—areas where existing approaches have encountered practical difficulties. These challenges highlight the need for sophisticated scheduling and resource management to fully realize the benefits of CPU-offloaded attention computation without introducing prohibitive costs or performance bottlenecks.

To address these challenges, we propose APEX, an LLM inference system that attempts to asynchronously overlap CPU and GPU calculations. Our primary contributions in APEX are:

1. We introduce an Asynchronous Overlap Execution mechanism that schedules CPU-computed attention results to hide CPU latency within unified GPU batches, eliminating batch splitting overheads.
2. We develop a decision mechanism for Asymmetric Pipelining, guided by an empirically-derived inequality (Section 3.2), to selectively apply pipelining only when beneficial.
3. We integrate these ideas into a performance-model-driven scheduler that dynamically adapts to workload and hardware characteristics based on offline profiling, maximizing throughput under memory constraints.

By treating the CPU as an active compute tier in the LLM inference pipeline, APEX introduces a new systems-level abstraction for heterogeneous, memory-aware scheduling that directly targets runtime and resource orchestration.

2 BACKGROUND AND MOTIVATION

Large Language Models (LLMs) are increasingly central to applications that generate extended, contextually rich text, from detailed Chain-of-Thought reasoning to nuanced multi-turn conversations. A critical challenge in deploying these powerful models, however, is the substantial GPU memory footprint of the KV cache, which grows linearly with sequence length during auto-regressive inference. This escalating memory demand severely constrains system throughput and the ability to co-locate multiple models or serve large batches. In response, hybrid CPU-GPU architectures have emerged, aiming to leverage capacious host DRAM for memory-intensive aspects of inference. While this approach holds considerable promise for alleviating GPU memory pressure, it introduces significant systems-level complexities in efficiently orchestrating computation and data across heterogeneous resources, particularly for latency-sensitive online services.

2.1 LLM Inference: Memory Pressure from KV Caches

Modern LLMs predominantly use the decoder-only transformer architecture [4, 12, 9]. Inference involves tokenizing input, embedding tokens, and then passing them through multiple transformer blocks. Each block typically contains a Multi-Head

Attention (MHA) mechanism and a Position-wise Feed-Forward Network (FFN), crucial for capturing contextual relationships and transforming representations. The process culminates in generating an output token, which is then fed back auto-regressively to produce the next token until a stopping condition is met.

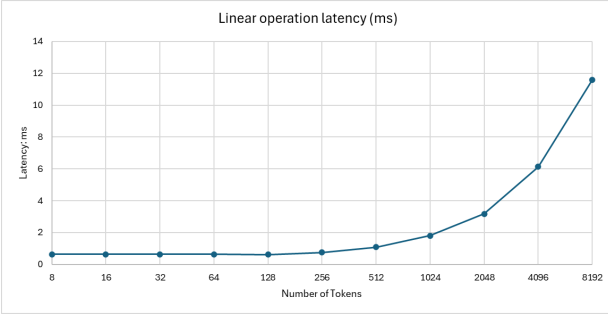
A critical aspect of this auto-regressive generation is the KV cache. During the MHA computation, Key (**K**) and Value (**V**) vectors are computed for each token at each layer. To avoid redundant computations in subsequent steps, these **K** and **V** vectors are cached. As the sequence length (N) grows, the KV cache size increases linearly (proportional to $N \times d_{model} \times \text{num_layers}$), consuming substantial GPU memory [20, 24]. For instance, LLaMa-65B on 4 A100 GPUs can generate KV cache at 13.9 GiB/s, quickly exhausting GPU memory [10]. This GPU memory footprint of the KV cache often becomes the primary limiting factor for the achievable batch size, thereby constraining overall throughput and GPU utilization, especially on memory-constrained devices [20, 32]. While attention variants like Multi-Query Attention (MQA) [25] and Grouped-Query Attention (GQA) [2] reduce KV cache size by sharing K/V projections, the fundamental challenge of managing a growing cache in limited GPU memory persists.

LLM inference is typically divided into two phases: *prefill*, processing the initial prompt, and *decode*, generating subsequent tokens one by one. The decode phase, often constituting the bulk of the generation time for long sequences, is particularly sensitive to KV cache management. Optimizations like kernel fusion and specialized attention kernels (e.g., FlashAttention [7] and its derivatives [6, 8, 14]) improve computational efficiency, primarily by reducing memory traffic to/from GPU memory. However, they do not fundamentally alleviate the GPU memory capacity bottleneck imposed by the KV cache itself.

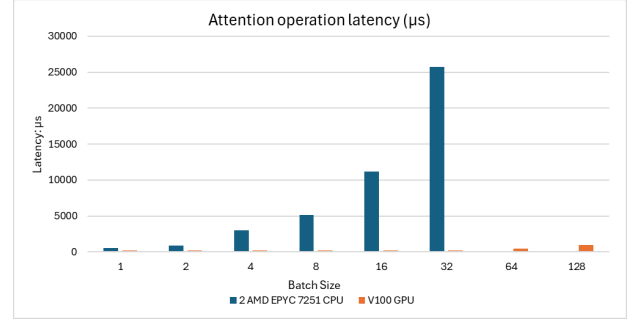
2.2 Hybrid CPU-GPU Inference: Opportunities and Pitfalls

The disparity between limited, expensive GPU memory and relatively abundant, cheaper host system DRAM (often terabytes in modern servers) motivates exploring hybrid CPU-GPU inference systems. Initial offloading strategies involved moving less frequently accessed model parameters or the entire KV cache to CPU memory, transferring them back to the GPU when needed [26, 9]. Frameworks like HuggingFace Accelerate and FlexGen [26] support such schemes. However, the KV cache is accessed at every decoding step. Consequently, frequently swapping large KV cache segments over the relatively slow CPU-GPU interconnect (e.g., PCIe) introduces significant latency, making these approaches unsuitable for latency-sensitive online inference [13, 26].

A more promising strategy is to offload only the *computation* of the decode-phase self-attention, along with its KV cache management, to the CPU, leveraging its attached high-capacity DRAM [13, 16]. This approach is compelling due to a confluence of factors that make CPU co-processing viable for this specific task. Central to its feasibility is the inherently memory-bandwidth-bound nature of the decoding attention process on both GPU and CPU architectures; this characteristic arises from its low arithmetic intensity (FLOPs per byte of memory accessed), meaning performance is dictated more by the speed of memory access to the extensive KV cache than by raw computational throughput [13, 39]. Compounding this, while GPUs



(a) Latency of linear operations (Q, K, V, O projections, FFNs) for one layer of LLaMa-3.1-8B on an A10 GPU, varying with the number of tokens computed.



(b) Attention latency for one LLM layer on a V100 GPU and two AMD EPYC 7251 CPUs, by batch size. CPU latencies at batch sizes 64 and 128 are not shown due to being substantially higher than GPU latencies.

Figure 1: Performance analysis of LLM operations. (a) Linear operation latency scaling with token count on an A10 GPU for LLaMa-3.1-8B. (b) Comparison of CPU vs. GPU attention latency across batch sizes.

maintain a significant advantage in peak floating-point operations, the disparity in memory bandwidth between high-end server CPUs and their GPU counterparts is considerably less pronounced. For instance, an NVIDIA A10G GPU might offer approximately 600 GB/s of memory bandwidth, whereas a modern server CPU can deliver a substantial fraction of this, in the order of 200 GB/s [13]. For operations like decode-phase attention, where performance is predominantly gated by memory access, this reduced bandwidth gap renders CPU execution a practical consideration. The primary advantage realized from such offloading is significant GPU memory relief; by shifting the memory-intensive attention workload, substantial GPU memory is liberated. This newly available memory can then be strategically reallocated to increase batch sizes for the compute-intensive linear operations (such as Feed-Forward Networks) that remain GPU-resident, thereby enhancing overall GPU utilization and potentially boosting system throughput, particularly under memory-constrained conditions.

However, this hybrid approach is not without pitfalls. Transferring token embeddings to the CPU and attention outputs back to the GPU incurs PCIe latency. Moreover, the CPU’s lower raw compute power means attention computation itself will be slower than on the GPU. Thus, realizing a net performance benefit hinges on sophisticated scheduling to effectively overlap CPU attention computation with GPU execution of other layers (e.g., FFNs) and hide these overheads.

2.3 State-of-the-Art in Hybrid CPU-GPU LLM Inference Scheduling

Early efforts in hybrid execution aimed to overcome GPU VRAM limitations and improve throughput by leveraging CPU resources. FastDecode [13] was among the first to demonstrate executing decode-phase self-attention on the CPU. It showed that for memory-bandwidth-bound attention, CPUs could sustain a reasonable fraction of GPU performance, thereby freeing valuable GPU memory. However, its evaluation primarily focused on scenarios with fixed input/output lengths and often assumed substantial, potentially costly, dedicated CPU resources (e.g., eight 32-core AMD Epyc CPUs for a single A10 GPU in some experiments). This reliance on extensive CPU parallelism might not

be practical or cost-effective for all deployment environments. Furthermore, its scheduling was less focused on dynamic adaptation to mixed prefill/decode workloads or achieving fine-grained computational overlap in highly variable online settings.

MOE-Lightning [5] also explored overlapping CPU attention with GPU computation. However, its primary context was offline inference for Mixture-of-Experts (MoE) models, where input and output lengths are often pre-determined, and the scheduling complexities differ from those of dynamic online LLM serving. Consequently, its techniques are less directly applicable to the latency-sensitive, interactive nature of online inference for general-purpose LLMs.

NEO [16] significantly advanced hybrid scheduling by considering both prefill and decode stages, proposing the Asymmetric Pipelining technique and a load-aware scheduler to manage the decomposed execution. While NEO can achieve performance gains, particularly when GPU memory is extremely constrained (forcing small GPU batches), its scheduler relies on a greedy, heuristic algorithm. This approach can lead to suboptimal decisions, failing to consistently maximize CPU-GPU computational overlap. In some situations, it may even result in performance degradation due to introduced overheads or miscalculations from the heuristic model. Critically, for decode-intensive workloads where prefill operations are infrequent or absent, NEO’s scheduler often defaults to a GPU-only execution mode or employs batch splitting for CPU offloading via Asymmetric Pipelining. As we will detail in Section 2.4, this batch splitting can introduce its own significant inefficiencies, potentially underutilizing CPU resources if not carefully managed. This leaves an un-addressed gap for scenarios common in chat applications or Chain-of-Thought reasoning, where decode phases are long and performance-critical.

These limitations in existing systems highlight a critical research opportunity: the need for a scheduling strategy that can dynamically and effectively overlap CPU-offloaded attention with GPU computation, specifically tailored for the decode phase of online inference workloads, especially those generating long output sequences. Such a scheduler must be profiling-informed to make accurate predictions, avoid the pitfalls of purely heuristic methods, and crucially, manage resources to maximize parallelism

without resorting to performance-degrading mechanisms like unnecessary batch splitting. This is precisely the gap APEX aims to fill.

2.4 The Decode-Only Bottleneck in Asymmetric Pipelining for Hybrid Inference

The Asymmetric Pipelining technique, proposed by NEO [16], is a valuable concept for hybrid execution. However, it faces a specific set of challenges when applied to workloads dominated entirely by decode requests, a common scenario in online inference for conversational or multi-step reasoning tasks. In these prefill-absent phases, where the system only incrementally generates tokens, the effectiveness of Asymmetric Pipelining diminishes due to several factors:

Impact of Batch Splitting on Linear Operations. A key observation from our profiling (illustrated in Figure 1a) is that the GPU computation time for linear operations (T_{linear} – e.g., Q, K, V, O projections, FFNs) remains relatively stable for the smaller batch sizes typical in decode-only phases (e.g., batch size < 256). Furthermore, GPUs benefit from processing decode requests in a single, larger batch to maximize utilization. Asymmetric Pipelining, by its design, splits an incoming decode batch into two smaller sub-batches to facilitate its pipeline (Figure 2). Consequently, the GPU executes linear operations twice per effective cycle (once for each sub-batch). This splitting often leads to a near doubling of the total time spent on these linear operations compared to processing the original batch monolithically on the GPU, negating potential benefits from parallelism.

Pipeline Underutilization. Our experiments further indicate that with Asymmetric Pipelining in decode-only workloads, the first sub-batch in the pipeline (intended for GPU-centric work and prefill) often contains few or no CPU-offloaded requests that could run in parallel on the CPU during that stage. If prefill is absent, this sub-batch may be lightly loaded overall, leading to pipeline underutilization or “bubbles.” This occurs due to inefficiencies in achieving consistent overlap when the workload does not naturally fit the two-sub-batch structure designed for mixed prefill-decode loads, diminishing the potential gains from CPU offloading.

CPU-GPU Performance Disparity. While offloading attention to the CPU can free up GPU memory, CPUs are significantly slower at the matrix operations central to attention than GPUs. Our empirical measurements, illustrated in Figure 1b (showing latency for a single LLM layer with hidden size 2048 and sequence length 1024 on a V100 GPU versus dual AMD EPYC 7251 CPUs), starkly highlight this disparity. For instance, at a batch size of 4, the CPU attention latency is over 3031 μ s compared to the GPU’s 170 μ s. This performance gap widens dramatically with increasing batch sizes, with CPU latency becoming orders of magnitude higher. Such data consistently shows that CPU attention performance is typically less than 10% of the GPU’s. This substantial performance difference makes it inherently difficult for CPU offloading via Asymmetric Pipelining to achieve a net speedup in decode-only settings, especially when considering the overheads from batch splitting and potential pipeline imbalances. A detailed analytical model supporting why this performance ratio is critical for achieving speedup with pipelining is presented in Section 3.2.

Therefore, the combined effects of increased linear operation time due to batch splitting, potential pipeline underutilization, and the substantial CPU-GPU performance gap pose significant challenges for Asymmetric Pipelining in delivering throughput improvements for decode-only workloads. These observations highlight the critical need for alternative strategies, like our proposed Asynchronous Overlap method (detailed in Section 3.3), which specifically targets these issues to enable effective CPU-GPU collaboration without the associated penalties.

3 APEX SYSTEM DESIGN

Building upon the limitations identified with existing approaches in decode-only scenarios, APEX (Asynchronous Parallel CPU-GPU Execution) introduces a novel scheduling strategy centered around an Asynchronous Overlap mechanism. This section details the overall system architecture and the core principles of this mechanism.

3.1 System Overview

The APEX system architecture, illustrated in Figure 3, is designed to dynamically manage and execute LLM inference requests by leveraging both GPU and CPU resources. It comprises several key components:

- **Offline Profiler and Performance Model:** Similar to NEO, APEX utilizes an offline profiler to gather execution times for various model components (e.g., linear operations, GPU/CPU attention) across different batch sizes and sequence lengths. This data informs a performance model used by the scheduler.
- **Request Queues:** Incoming prefill and decode requests are managed in separate queues.
- **Dynamic Scheduler:** At each iteration, the scheduler selects requests from the queues and, based on the performance model, system state (e.g., GPU memory availability), and the nature of the requests (prefill vs. decode), decides on the optimal execution strategy. Strategies include GPU-only execution, Asymmetric Pipelining (governed by Inequality (5)), and our novel Asynchronous Overlap mechanism.
- **KV Cache Management:** KV cache management is handled dynamically according to the chosen execution strategy. GPU memory is utilized to cache KV pairs for requests being actively processed on the GPU, maximizing its batching capability.

The core innovation of APEX lies in its Asynchronous Overlap mechanism, designed specifically to enhance performance during decode-intensive phases.

3.2 Analytical Model for Scheduling Decisions

To determine when offloading decode requests to the CPU via pipelining is beneficial, particularly for deciding whether to use the Asymmetric Pipelining strategy in decode-only scenarios, APEX employs an analytical model. This model helps APEX’s scheduler (detailed in Algorithm 1) decide whether conditions favor Asymmetric Pipelining or if an alternative, such as our

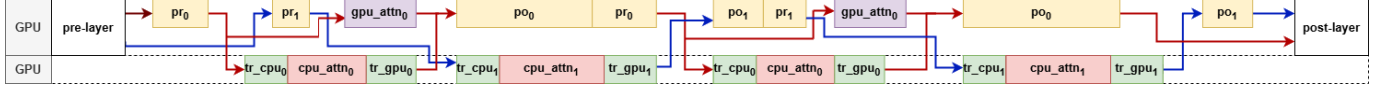


Figure 2: Asymmetric pipelining split the requests into two sub-batches. The first sub-batch (red arrows) contains prefilling and GPU/CPU decoding requests. The second sub-batch (blue arrows) contains only CPU decoding requests. “pr” means pre-projection, while “po” means post-projection + FFN operations; “attn” means attention operations; “tr” means transfer of intermediate value to GPU/CPU.

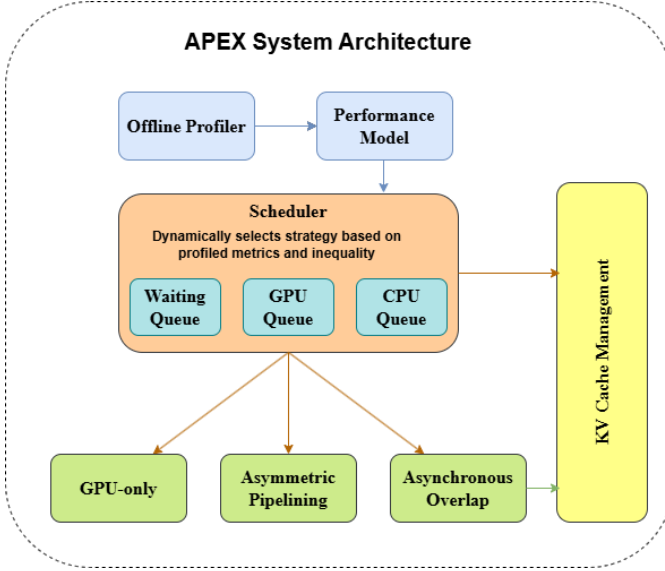


Figure 3: APEX System Architecture

proposed Asynchronous Overlap mechanism, is more appropriate.

Let N_G be the rate (tokens per unit time) at which the GPU processes self-attention, and N_C be the rate for the CPU. $T_{glinear}$ represents the GPU computation time for the linear operations within a transformer layer for a given batch size in the decode phase, and T_{gatt} denotes the GPU computation time for the self-attention operation for that same batch. For this derivation, data transfer times are excluded to focus on the computational trade-offs.

For a GPU-only execution handling a batch of decode requests, the time per iteration ($T_{gpuonly}$) is:

$$T_{gpuonly} = T_{glinear} + T_{gatt} \quad (1)$$

In an Asymmetric Pipelining scenario tailored for decode-only requests, the pipeline structure involves two sub-batches. Due to batch splitting, the linear operations are effectively performed twice in terms of impact on the cycle time. Thus, the effective cycle time ($T_{overlap}$) is estimated as:

$$T_{overlap} \approx 2T_{glinear} + T_{gatt} \quad (2)$$

Within this pipelined execution, the number of tokens processed by the GPU’s attention mechanism in its segment of the pipeline is:

$$N_{Gtotal} = N_G \times T_{gatt} \quad (3)$$

The number of tokens processed by the CPU’s attention mechanism, operating for the duration $T_{overlap}$ in its segment of the

pipeline, is:

$$N_{Ctotal} = N_C \times T_{overlap} = N_C(2T_{glinear} + T_{gatt}) \quad (4)$$

The throughput for the Asymmetric Pipelining system in this decode-only context is $\frac{N_{Gtotal} + N_{Ctotal}}{T_{overlap}}$. For the GPU-only case, to process a comparable unit of N_{Gtotal} tokens (representing the GPU’s attention work), the throughput is $\frac{N_{Gtotal}}{T_{gpuonly}}$. For Asymmetric Pipelining to provide a speedup over a GPU-only approach for this decode workload, its throughput must be higher:

$$\frac{N_G T_{gatt} + N_C(2T_{glinear} + T_{gatt})}{2T_{glinear} + T_{gatt}} > \frac{N_G T_{gatt}}{T_{glinear} + T_{gatt}} \quad (5)$$

Performing algebraic transformations on Inequality (5), we arrive at the condition required for Asymmetric Pipelining to be beneficial:

$$\frac{N_G}{N_C} < 2 \frac{T_{glinear}}{T_{gatt}} + 3 + \frac{T_{gatt}}{T_{glinear}} \quad (6)$$

This Inequality (6) is crucial for APEX’s scheduler. It indicates that the effectiveness of Asymmetric Pipelining for decode-only batches depends on the GPU-to-CPU attention speed ratio (N_G/N_C) and the system’s characteristic ratio of linear operation time to attention time ($T_{glinear}/T_{gatt}$). For typical $T_{gatt}/T_{glinear}$ ratios (between 0.5 and 1.5), N_G/N_C must generally be less than ~ 7.5 . This implies CPU attention speed (N_C) must be at least $\sim 13\%$ of GPU attention speed (N_G) for this pipelining strategy to compensate for its overheads.

Given that empirical measurements show N_C is often less than 10% of N_G (as noted in Section 2.4), Inequality (6) is rarely satisfied in decode-only scenarios. Thus, this model guides the APEX scheduler to employ Asymmetric Pipelining for decode-only batches sparingly, only when the condition holds, and to otherwise prefer strategies like Asynchronous Overlap. For mixed workloads involving prefill, a modified version of this inequality (as detailed in Algorithm 1) is used, accounting for the different timing characteristics.

3.3 Asynchronous Overlap Mechanism

We propose the Asynchronous Overlap mechanism to eliminate the need for a separate CPU-only sub-batch in decode-centric workloads and to improve CPU-GPU parallelism. Our approach integrates CPU decoding requests with GPU requests by processing them in a unified batch during the pre-attention operations (linear layers) for each transformer layer i ($i \in [1, num_layers]$). This unified processing for linear operations on the GPU avoids the doubling of $T_{glinear}$ discussed in Section 2.4 and leverages the GPU’s inherent efficiency in handling larger batches for these compute-bound tasks. Following these shared pre-attention computations, the processing path bifurcates: the query (Q), key (K),

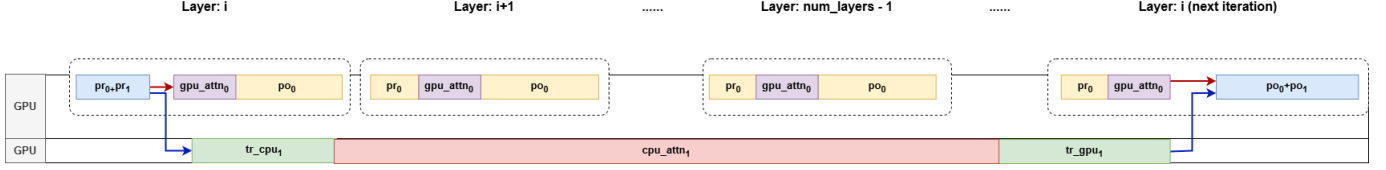


Figure 4: Asynchronous Overlap split the requests into two sub-batches. The first sub-batch (red arrows) contains prefilling and GPU decoding requests. The second sub-batch (blue arrows) contains only CPU decoding requests. The blue block indicates the synchronization point of GPU/CPU requests. “pr” means pre-projection, while “po” means post-projection + FFN operations; “attn” means attention operations; “tr” means transfer of intermediate value to GPU/CPU.

and value (V) tensors for requests designated for CPU attention are transferred to CPU memory. The GPU then proceeds with self-attention computations for its assigned requests, while the CPU concurrently computes self-attention for the offloaded requests.

The key innovation in Asynchronous Overlap is the strategic scheduling of result synchronization. Rather than immediately returning CPU-computed self-attention results to the GPU upon their completion (i.e., when the GPU might be ready to begin post-attention operations for layer i), we deliberately delay this transfer. The CPU-computed attention results for layer i are only required to be transferred back to the GPU and synchronized just before the GPU needs them to begin its post-attention linear operations for that same layer i in the *subsequent* processing cycle of the batch, as illustrated conceptually in Figure 4.

This design leads to two key advantages. Primarily, it facilitates a maximized CPU compute window. The delayed synchronization provides the CPU with a significantly extended window to perform its attention computations. Unlike Asymmetric Pipelining, where CPU overlap is primarily confined to the GPU’s attention phase, our Asynchronous Overlap allows the CPU’s compute window for a given layer’s attention to span the GPU’s execution of its own pre-attention linear layers, its self-attention computations across all layers, and its post-attention linear layers for the current iteration. This effectively gives the CPU the entire duration of the GPU’s iteration cycle to complete its offloaded attention tasks for a specific layer before synchronization is required for that layer in the next cycle.

Secondly, this approach results in reduced pipeline bubbles and consequently enhanced GPU utilization. The single, strategically deferred synchronization per layer, per full iteration cycle for a batch, offers a much longer and more flexible period for CPU tasks. This design minimizes the likelihood of the CPU becoming a critical-path bottleneck or the GPU waiting idly for CPU results. In contrast, experimental observations with Asymmetric Pipelining show that its two-sub-batch structure can lead to inefficiencies; specifically, the first sub-batch (which may include prefill requests) often contains no CPU-offloaded decode requests, effectively creating a “bubble” where CPU resources dedicated to that sub-batch’s pipeline stage are underutilized. Asynchronous Overlap mitigates such bubbles by ensuring the CPU has a continuous and substantial workload derived from the unified batch.

By synchronizing only once per iteration at a non-critical juncture relative to the GPU’s timeline, and by processing linear operations on a unified batch, Asynchronous Overlap aims to achieve a more effective and sustained overlap of CPU and GPU

computation. This approach is particularly beneficial in decode-heavy workloads. Even if CPU attention is slower per token than GPU attention, it can contribute significantly to overall throughput if provided with a sufficiently long and uninterrupted execution window, as facilitated by this mechanism. The scheduler (detailed in Section 3.4) determines when to employ this Asynchronous Overlap strategy, typically when Inequality (5) suggests that Asymmetric Pipelining would not be beneficial for the current batch of decode-only requests.

3.4 Scheduling Algorithm

The scheduler determines which requests to run in the current iteration and which strategy to choose. Our scheduling algorithm follows several key principles designed to optimize the balance between GPU and CPU processing:

The scheduler follows four primary rules:

- **GPU-first approach:** Consider CPU involvement only if GPU memory cannot hold KV caches for all new requests. When the GPU can handle all requests simultaneously, there is no benefit in involving the CPU due to the GPU’s substantially higher computing power.
- **Decode-only optimization:** With only decoding requests present, the scheduler evaluates inequality (6) to determine whether asymmetric pipelining would provide speedup compared to a GPU-only strategy. At this point, GPU memory is typically fully utilized, so $T_{glinear}$ and T_{gatt} remain stable. The scheduler need only calculate how many tokens the CPU can process within the time window $2T_{glinear} + T_{gatt}$. If the inequality holds, the scheduler selects asymmetric pipelining; otherwise, it switches to asynchronous overlap.
- **Mixed workload handling:** With both prefilling and decoding requests present, the scheduler applies a modified version of the inequality. Although prefilling requests exist, the comparison still focuses on CPU decoding versus GPU decoding speeds, as prefilling and decoding have different per-token processing times that cannot be directly compared. The values N_G , T_{gatt} , and $T_{glinear}$ remain unchanged since GPU decoding speed is fixed. However, equation (4) changes to $N_{Ctotal} = N_C(T_{glinear_with_prefill} + T_{glinear} + T_{gatt_with_prefill})$. In this scenario, the CPU has more time to process tokens, making speedup more achievable.
- **Partial progress prioritization:** When using asynchronous overlap, if some CPU requests have already

completed the first i layers of decoding when new pre-filling requests arrive, and the inequality holds, the scheduler prioritizes these partially processed CPU requests in the decode-only sub-batch if the other sub-batch is full. This optimization is valuable because these requests add only $(num_layers - i) \cdot T_{glinear}$ extra time instead of $num_layers \cdot T_{glinear}$ extra time.

Algorithm 1: APEX Scheduling Algorithm

Input : Prefill request queue P_{in} , GPU Decode request queue D_{gpu_in} , CPU Decode request queue D_{cpu_in} (populated based on KV cache availability on GPU), GPU processing speed N_G , CPU processing speed N_C

Output : Scheduled requests and execution strategy for the current iteration

$P_{sch} \leftarrow$ Select active prefill requests from P_{in} ;
 $D_{gpu_sch} \leftarrow$ Select active decode requests from D_{gpu_in} ;
 $D_{cpu_sch} \leftarrow$ Select active decode requests from D_{cpu_in} ;
if D_{cpu_sch} *is empty* **then**
 return GPU-only strategy for D_{gpu_sch} requests;
 ▷ No requests designated for CPU offload
end
 $T_{glinear} \leftarrow$ Profiled GPU linear operation time (decode-only);
 $T_{gatt} \leftarrow$ Profiled GPU self-attention time (decode-only);
if P_{sch} *is empty* **then**
 ▷ Decode-only scenario. Refers to Inequality (5)
 if $\frac{N_G T_{gatt} + N_C (2T_{glinear} + T_{gatt})}{2T_{glinear} + T_{gatt}} > \frac{N_G T_{gatt}}{T_{glinear} + T_{gatt}}$ **then**
 return Asymmetric Pipelining strategy for D_{gpu_sch} and D_{cpu_sch} ;
 else
 return Asynchronous Overlap strategy for D_{gpu_sch} and D_{cpu_sch} ;
 end
end
else
 ▷ Mixed prefill and decode scenario
 $T_{glinear_pref} \leftarrow$ Profiled GPU linear operation time (with prefill);
 $T_{gatt_pref} \leftarrow$ Profiled GPU self-attention time (with prefill);
 $T_{overlap_with_prefill} \leftarrow T_{glinear_pref} + T_{glinear} + T_{gatt_pref}$;
 if $\frac{N_G T_{gatt} + N_C T_{overlap_with_prefill}}{2T_{glinear} + T_{gatt}} > \frac{N_G T_{gatt}}{T_{glinear} + T_{gatt}}$ **then**
 Partition $P_{sch}, D_{gpu_sch}, D_{cpu_sch}$ for Asymmetric Pipelining;
 Prioritize partially processed requests from D_{cpu_sch} in the CPU-only sub-batch;
 return Asymmetric Pipelining strategy with partitioned requests;
 else
 return Asynchronous Overlap strategy for $P_{sch}, D_{gpu_sch}, D_{cpu_sch}$;
 ▷ Asynchronous Overlap adapted for mixed workloads
 end
end

The APEX scheduling procedure, detailed in Algorithm 1, dynamically adapts to workload characteristics, optimizing resource allocation between the GPU and CPU to maximize throughput while preserving latency. A key aspect of its robustness, particularly within the Asynchronous Overlap strategy, involves managing CPU-GPU synchronization. Before the desig-

nated synchronization point (i.e., prior to the GPU commencing post-attention operations for a given layer), the GPU checks if the CPU’s offloaded computation for that layer is complete. If the CPU results are not yet ready, the GPU does not stall; instead, it proceeds with its current tasks for the ongoing iteration. The GPU will re-check for CPU readiness in the subsequent iteration, repeating this check until the CPU results are available for synchronization.

4 IMPLEMENTATION

We implement APEX by extending the open-source NEO system. Our implementation introduces two key contributions: (1) a new CPU paged attention backend built on Llamafile, (2) a multi-threaded runtime using Pybind11 to enable asynchronous GPU-CPU overlap.

4.1 Integration of Llamafile Kernels

Neo implement a custom Paged Attention kernel for CPU with ISPC (ispc/ispc)—a language for writing SPMD programs on CPU. Instead, we implement the Paged Attention kernel for CPU with Llamafile Matrix Multiplication Kernel. Llamafile is a Mozilla open source project which combine llama.cpp with Cosmopolitan Libc into one framework that collapses all the complexity of LLMs down to a single-file executable (called a “llamafile”) that runs locally on most computers, with no installation. It provides efficient matrix multiplication kernels for CPU adopted by llama.cpp and ktransformers. We implement our version of CPU paged attention with llamafile matrix multiplication kernel. In such case, the CPU paged attention speed reduce a little when batch size is small compared to Neo custom paged attention. Consequently, as the batch size expands, our CPU paged attention achieves speeds up to twice that of Neo’s custom paged attention. This enhanced CPU performance significantly expands the opportunities to effectively overlap CPU paged attention computations with concurrent GPU operations.

4.2 Asynchronous GPU-CPU Overlap Runtime

To achieve asynchronous overlap between CPU and GPU operations, our system employs a two-threaded Python architecture. The main thread manages core system logic and initiates CUDA kernel launches for GPU tasks, while a dedicated compute thread executes CPU-bound attention operations. To enable true parallelism despite Python’s Global Interpreter Lock (GIL), we integrate C++ routines for attention computations using Pybind11 with the `gil_scoped_release` attribute; this allows the GIL to be released during C++ execution, permitting concurrent GPU task dispatch by the main thread. While this strategy facilitates the desired overlap, Python thread contention and scheduling overheads are inherently present. Consequently, the CPU compute thread must process a sufficient volume of requests in each iteration to effectively amortize these overheads. We therefore establish a minimum threshold for the number of CPU requests required to initiate CPU-based attention computations. Our empirical evaluations indicate that these overheads are adequately offset when the quantity of CPU requests is at least eight times greater than that of GPU requests.

CPU(cores)	RAM	GPU
2 Xeon 6342(2*24 cores)	250GB	Nvidia A10
2 Xeon 6130(2*16 cores)	180GB	Nvidia T4

Table 1: Hardware Settings of Our Experiments

5 EVALUATION

5.1 Experiment Setup

Testbed.. We run our experiments on two different systems: (1) dual Intel Xeon Gold 6342 processors (2.80GHz, 24 cores per processor) with an NVIDIA A10 GPU, and (2) dual Intel Xeon Gold 6130 CPUs (2.10GHz, 16 cores per processor) with an NVIDIA T4 GPU. The hardware characteristics of our experiment settings are shown in Table 1.

Models.. We evaluate LLaMa-2-7B on the T4 platform and LLaMa-3.1-8B on the A10 platform; these pairings ensure model-to-GPU memory compatibility (LLaMa-2-7B with T4’s 16GB GPU memory; LLaMa-3.1-8B with A10’s 24GB GPU memory) and reflect distinct, realistic hardware deployment scenarios based on resource constraints and performance requirements for each model size.

Baseline. We compare APEX with 2 baselines listed below:

- **vLLM** is one of the state-of-the-art high-throughput and memory-efficient inference and serving engine for LLMs aiming for high-end GPUs.
- **SwiftLLM** is a tiny yet powerful LLM inference system tailored for researching purpose. It gains vLLM-equivalent performance with only 2k lines of code on single GPU.
- **NEO** is a LLM inference engine built to save the GPU memory crisis by CPU offloading. We built our system based on Neo.

Workloads. We use several real world workloads for different tasks.

- Azure LLM inference trace for conversation (Azure Conversation) is a sample of the traces from multiple LLM inference services in Azure, collected on May 10th-19th 2024.
- LiveBench is a benchmark for LLMs designed with test set contamination and objective evaluation in mind.
- Dolphin-r1 is a 800k sample dataset similar in composition to the one used to train DeepSeek-R1 Distill models.
- The OpenAI Summarization Comparison (OSC) dataset is a publicly available resource comprising input texts, each paired with a human-selected (‘chosen’) summary and a ‘rejected’ alternative, all originating from real-world interactions between humans and a chatbot.

5.2 Throughput

We conducted throughput evaluations of APEX against baseline systems on both A10 and T4 GPU architectures, with results presented in Figure 5. On the A10 GPU, APEX demonstrated significant performance improvements across three benchmark workloads: LiveBench (6% improvement over NEO, 22% over vLLM), Azure Conversation (13% over NEO, 11% over vLLM), and Dolphin-r1 (16% over NEO, 20% over vLLM). These results indicate consistent throughput gains for APEX across diverse workload characteristics.

For the T4 GPU evaluation, we employed the OSC workload and varied the average output length. Under this configuration, APEX achieved significantly higher throughput, outperforming NEO by up to 71% and vLLM by up to 96%.

The observed speedup is primarily attributed to APEX’s ability to effectively overlap CPU and GPU computations, particularly during decode-intensive phases of request processing. The magnitude of this speedup is influenced by two principal factors: first, the computational power disparity between the GPU and CPU, and second, the proportion of the total execution time occupied by these decode-intensive phases. Theoretically, if we denote the ratio of GPU to CPU computational power as a and the ratio of decode-intensive time to total time as b , the achievable speedup S can be approximated by: $S \approx \frac{b}{a}$.

The more substantial throughput improvements observed on the T4 platform, compared to the A10, can be explained by these factors. The T4 GPU possesses considerably lower computational power relative to the A10 GPU (resulting in a smaller value for a). However, the CPU processing capabilities were comparable across both experimental setups. Furthermore, the OSC workload, used in the T4 experiments, inherently features a larger proportion of decode-intensive time (a larger b) compared to the workloads deployed on the A10. Consequently, the combination of a less powerful GPU (smaller a) and a workload with a higher ratio of decode-dominant operations (larger b) collectively contributes to the more pronounced speedup achieved by APEX on the T4 GPU.

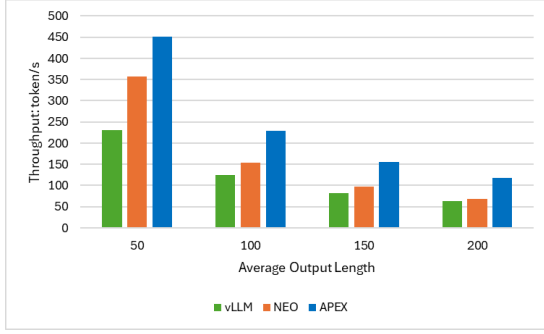
5.3 Average Per Token Latency

In addition to throughput, we evaluated the average per-token latency of APEX in comparison to vLLM and NEO on both T4 and A10 GPUs. The results, presented in Figure 6, demonstrate notable latency advantages for APEX. Specifically, on the T4 GPU, APEX achieved nearly half the average per-token latency observed with NEO. On the A10 GPU, APEX also exhibited a slightly smaller latency compared to NEO.

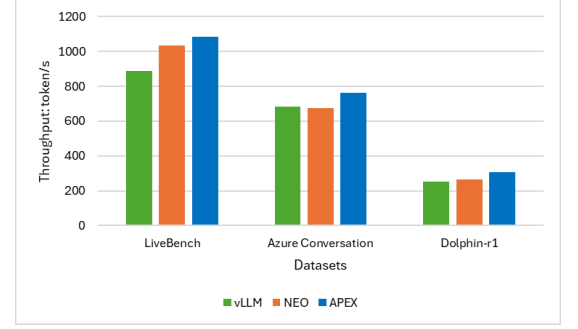
Considering these latency results in conjunction with our throughput experiments, it is evident that APEX not only achieves higher throughput than NEO but also maintains comparable or even superior latency performance.

5.4 Varying Output Lengths

To further elucidate the performance characteristics of APEX, particularly in relation to the average output length of generated sequences, we conducted a dedicated evaluation on the A10 GPU. We normalize all throughput values to SwiftLLM to establish a consistent GPU-only baseline. In this experiment, the

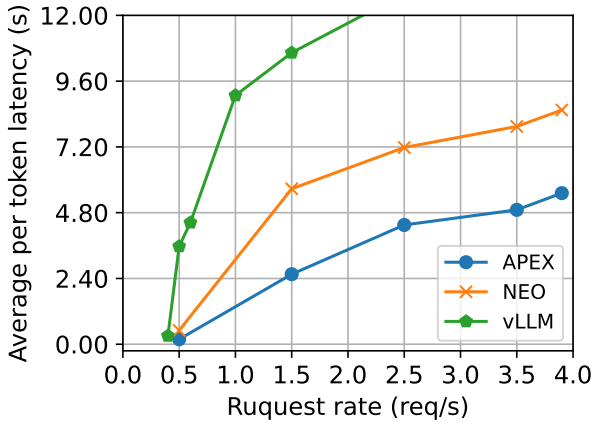


(a) T4 + LLaMa-2-7B + OSC with varied average output length

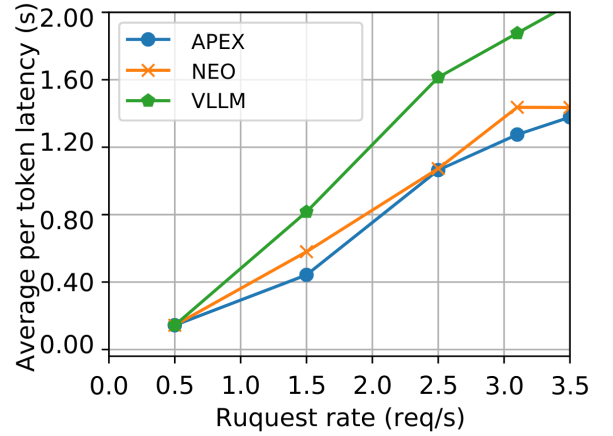


(b) A10 + LLaMa-3.1-8B + 3 workloads (Azure Conversation, LiveBench, Dolphin-r1)

Figure 5: Throughput in different GPUs and different synthetic workloads



(a) T4 + LLaMa-2-7B + OSC



(b) A10 + LLaMa-3.1-8B + AC.

Figure 6: Average per token latency curve comparison between NEO, vLLM and APEX on T4 and A10 GPUs. For each request, we compute its per-token latency by dividing its full latency by its output token number, and then we take the average among all requests.

average output length was systematically varied, and the results, depicted in Figure 7, align closely with our previously discussed theoretical framework regarding CPU-GPU computation overlap.

The data reveals distinct performance trends based on output length. When the average output length is relatively short (ranging from 50 to 200 tokens), APEX demonstrates a modest throughput advantage (5%) over NEO. In such scenarios, the overall execution time is significantly influenced by the initial prefill stage and a mixture of prefill and decode operations, rather than being dominated by extended decode-intensive phases. Consequently, the opportunities for APEX to leverage CPU-GPU parallelism for speedup are less pronounced.

As the average output length increases (between 200 and 500 tokens), the performance gap between APEX and NEO widens progressively (17%, 22%, 31%). This trend is attributed to the increasing proportion of time spent in the decode phase, where APEX’s architecture excels. For average output lengths exceeding 500 tokens, decode-intensive operations constitute the majority of the processing time. In this regime, APEX achieves its

maximum observed benefit, realizing up to 37% higher throughput compared to NEO.

Notably, once the average output length becomes sufficiently long (e.g., above 600 tokens), the throughput advantage of APEX over NEO tends to stabilize. This plateau effect is consistent with our theoretical model: the maximum achievable speedup becomes constrained by the inherent ratio of GPU to CPU computational power. At this point, even with longer decode phases, the system reaches a steady state where the speedup is dictated by this fundamental hardware characteristic, as previously theorized by the relationship $S \approx \frac{b}{a}$, where the proportion of decode-intensive time (b) has maximized its contribution relative to the fixed compute power ratio (a). This underscores that while APEX significantly optimizes decode-heavy workloads, the ultimate performance ceiling is influenced by the underlying hardware balance.

6 DISCUSSION

Comparison with NEO. The APEX system utilizes the Asymmetric Pipelining technique, originally proposed by NEO, en-

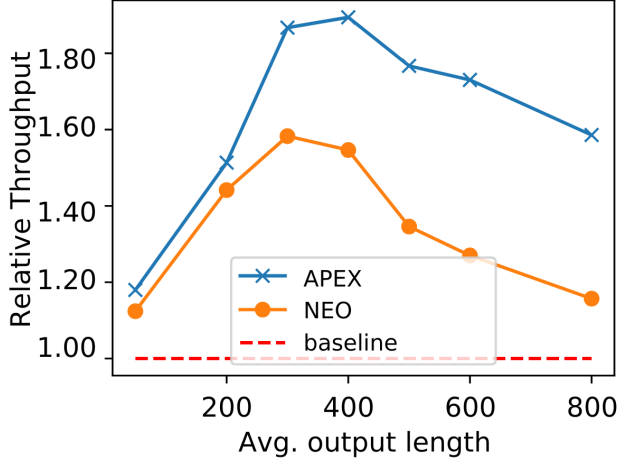


Figure 7: Relative throughput in varied average output length compared with SwiftLLM (GPU-only) as the baseline. The average input length is 1000.

hancing its effectiveness through a more sophisticated activation strategy. A key distinction in APEX’s approach is the deployment of a specific inequality criterion to precisely determine when Asymmetric Pipelining will be beneficial for the current workload. We have found this criterion to be more accurate in predicting actual speedup compared to methods relying solely on broader metrics, such as overall requests per second. This targeted strategy is designed to comprehensively identify opportunities where Asymmetric Pipelining can yield performance benefits, while concurrently minimizing scenarios where its application might inadvertently lead to slowdowns. Furthermore, in instances where our inequality criterion indicates that Asymmetric Pipelining is unlikely to provide a speedup, APEX is architected to leverage an alternative optimization, Asynchronous Overlap, to pursue performance gains.

Pipeline Parallelism Support. The asynchronous decode approach faces a timing constraint: after CPU completes self-attention calculations for layer i , it must wait until the GPU returns to process layer i in the next iteration before transferring the results. With all layers executing sequentially on a single GPU, this creates substantial idle time for completed CPU computations.

Pipeline parallelism directly addresses this inefficiency by reducing the “cycle time” between consecutive processing of the same layer. When L layers are distributed across N devices (with each device handling L/N layers), the CPU only needs to wait for the completion of L/N layers rather than all L layers before its computations can be integrated back into the pipeline. This shortened cycle time dramatically reduces CPU waiting periods, allowing for more effective resource utilization and improved throughput in the asynchronous decode process.

For example, with an 80-layer model distributed across 8 GPUs (10 layers per device), the CPU’s waiting period is reduced by 75% compared to single-GPU execution, creating more opportunities for effective CPU-GPU collaboration and further enhancing the performance benefits of our asynchronous overlap strategy. We leave this as a future work.

CPU Attention Task Pool for Enhanced Flexibility. Currently, for operational efficiency, APEX processes CPU attention requests in batches, handling all requests for a single layer within one iteration. Looking ahead, we propose the development of a CPU attention computation task pool. As new requests arrive, they could be dynamically added to this pool. The CPU could then service these tasks, potentially with a layer-wise prioritization scheme (e.g., processing from the final layer back to the initial layer, or another heuristic based on computational cost or data dependencies). Such a system would enable the CPU to handle tasks from multiple layers within a single processing iteration. This could significantly reduce CPU idle time and improve overall resource utilization. However, this advanced scheduling would necessitate additional memory for storing intermediate values (e.g., residuals, outputs) from different layer tasks, thereby increasing both engineering complexity and the system’s memory footprint.

Improving Performance Predictability with Online Profiling. Our experiments revealed that offline profilers occasionally fail to accurately predict execution times for specific sequence lengths and batch sizes. These inaccuracies can negatively impact the efficiency of the CPU-GPU overlap, a core feature of APEX. For instance, if the actual CPU computation time exceeds the profiled prediction, the CPU can become a bottleneck, leading to GPU under-utilization. While comprehensive online profiling across all operational scenarios would likely incur prohibitive overhead, a more targeted approach is feasible. We envision implementing online profiling specifically for decode-intensive scenarios. In this context, the system could dynamically monitor CPU and GPU computation times. If the CPU computation time is observed to be consistently greater than that of the GPU for these decode tasks, APEX could then adaptively reduce the number of CPU-bound requests being processed concurrently, thereby rebalancing the workload to sustain optimal GPU utilization and overall throughput.

7 RELATED WORK

The imperative to deploy Large Language Models (LLMs) for online inference within GPU memory constraints has driven investigations into distributing workloads across CPU and GPU resources. While foundational optimizations for GPU-centric inference are well-established, this section reviews prior art in hybrid execution models and their approaches to managing offloaded computations, particularly the KV cache and attention mechanism.

Early forays into offloading for LLM inference primarily aimed to overcome GPU memory limitations by moving model parameters or the entire KV cache to more abundant CPU memory or even disk storage. Systems like FlexGen [26] pioneered dynamic offloading across a memory hierarchy, demonstrating the feasibility of running models exceeding GPU capacity. Similarly, inference engines such as llama.cpp [11] enable execution on CPU-centric or SSD-assisted setups. However, these general offloading strategies, when applied to the frequently accessed KV cache during the decode phase, often lead to prohibitive latencies due to repetitive data transfers over the PCIe bus, rendering them less suitable for low-latency online services [26]. Attempts to mitigate this through algorithmic I/O reduction, such as sparsity-based selective loading in LLMFlash [3] and

PowerInfer [27, 33], offer partial solutions but are often model-dependent and may not address the core challenge of coordinating active computations across heterogeneous processors during the decode phase.

Recognizing these bottlenecks, a more targeted approach of hybrid execution for the decode-phase attention mechanism has gained traction. This involves offloading the KV cache and the associated attention computation to the CPU, while retaining compute-intensive MLP layers on the GPU [13, 16]. Systems like FastDecode [13] and NEO [16] exemplify this principle. FastDecode demonstrated significant throughput by leveraging substantial (often remote) CPU resources to process attention computations in parallel with GPU tasks. NEO introduced a load-aware scheduler to manage the decomposed execution. These systems validated the architectural concept of CPU-based attention for freeing GPU memory and its particular relevance for deploying LLMs on resource-constrained edge hardware [12, 28, 1]. The broader exploration of inference optimization on diverse hardware, including various accelerators and Processing-in-Memory (PIM) devices [17, 18, 22, 37, 23], also underscores the general need for intelligent workload management in heterogeneous environments.

Despite these advancements in architecting hybrid execution, a critical gap remains in the effective scheduling and fine-grained overlap of CPU-offloaded attention tasks with ongoing GPU computations during the latency-sensitive, bandwidth-bound decode phase. Simply offloading attention is insufficient if the coordination between CPU and GPU introduces new stalls or fails to exploit available parallelism. For instance, the reliance of FastDecode [13] on extensive CPU parallelism highlights a potential resource scalability issue rather than an optimal co-scheduling solution for typical memory-constrained single-server setups. Furthermore, the heuristic and greedy nature of schedulers in systems like NEO [16] can lead to suboptimal decisions, failing to consistently maximize resource utilization or adapt to the dynamic characteristics of online workloads, such as those found in multi-turn conversations or reasoning tasks. This often results in underutilization of either the CPU or GPU, limiting the practical throughput gains anticipated from hybrid execution. Existing solutions have thus primarily focused on the mechanism of offloading, with less emphasis on dynamic, performance-aware scheduling to hide CPU latency and ensure continuous GPU operation during the decode phase.

Our work, APEX, directly addresses this scheduling deficiency. By introducing a performance-model-driven strategy, APEX is specifically designed to maximize CPU-GPU parallelism during the decode phase of hybrid LLM inference, thereby improving resource utilization and overall efficiency for online applications on memory-constrained GPUs.

8 CONCLUSION

We present APEX, a novel, performance-model-driven scheduling strategy designed to maximize CPU-GPU parallelism for online Large Language Model (LLM) inference on memory-constrained GPUs. APEX predicts CPU and GPU subtask execution times to dynamically dispatch computations, featuring an innovative Asynchronous Overlap method that effectively hides CPU latency without batch splitting overheads. We evalu-

ated APEX with LLaMa-2-7B and LLaMa-3.1-8B models on NVIDIA T4 and A10 GPUs. Experimental results demonstrate that APEX improves throughput by 84%-96% (T4) and 11%-89% (A10) over the GPU-only vLLM, and achieves up to 49% (T4) and 37% (A10) higher throughput than the state-of-the-art hybrid scheduler NEO in long-output settings, all while maintaining or improving average per-token latency.

REFERENCES

- [1] Marah Abdin, Jyoti Aneja, Hany Awadalla, Ahmed Awadallah, Ammar Ahmad Awan, Nguyen Bach, Amit Bahree, Arash Bakhtiari, Jianmin Bao, Harkirat Behl, Alon Benhaim, and et al. 2024. Phi-3 Technical Report: A Highly Capable Language Model Locally on Your Phone. *arXiv preprint arXiv:2404.14219* (2024).
- [2] Joshua Ainslie, James Lee-Thorp, Michiel de Jong, Yury Zemlyanskiy, Federico Lebrón, and Sumit Sanghai. 2023. GQA: Training Generalized Multi-Query Transformer Models from Multi-Head Checkpoints. *arXiv preprint arXiv:2305.13245* (2023).
- [3] Keivan Alizadeh, Iman Mirzadeh, Dmitry Belenko, Karen Khatamifard, Minsik Cho, Carlo C Del Mundo, Mohammad Rastegari, and Mehrdad Farajtabar. 2024. LLM in a flash: Efficient Large Language Model Inference with Limited Memory. *arXiv preprint arXiv:2312.11514* (2024).
- [4] Tom Brown, Benjamin Mann, Nick Ryder, Melanie Subbiah, Jared D Kaplan, Prafulla Dhariwal, Arvind Neelakantan, Pranav Shyam, Girish Sastry, Amanda Askell, Sandhini Agarwal, Ariel Herbert-Voss, Gretchen Krueger, Tom Henighan, Rewon Child, Aditya Ramesh, Daniel Ziegler, Jeffrey Wu, Clemens Winter, Chris Hesse, Mark Chen, Eric Sigler, Mateusz Litwin, Scott Gray, Benjamin Chess, Jack Clark, Christopher Berner, Sam McCandlish, Alec Radford, Ilya Sutskever, and Dario Amodei. 2020. Language Models are Few-Shot Learners. In *Advances in Neural Information Processing Systems*, H. Larochelle, M. Ranzato, R. Hadsell, M.F. Balcan, and H. Lin (Eds.), Vol. 33. Curran Associates, Inc., 1877–1901. https://proceedings.neurips.cc/paper_files/paper/2020/file/1457c0d6bfc4967418bfb8ac142f64a-Paper.pdf
- [5] Shiyi Cao, Shu Liu, Tyler Griggs, Peter Schafhalter, Xiaoxuan Liu, Ying Sheng, Joseph E. Gonzalez, Matei Zaharia, and Ion Stoica. 2025. MoE-Lightning: High-Throughput MoE Inference on Memory-constrained GPUs. In *Proceedings of the 30th ACM International Conference on Architectural Support for Programming Languages and Operating Systems, Volume 1* (Rotterdam, Netherlands) (ASPLOS '25). Association for Computing Machinery, New York, NY, USA, 715–730. <https://doi.org/10.1145/3669940.3707267>
- [6] Tri Dao. 2023. FlashAttention-2: Faster Attention with Better Parallelism and Work Partitioning. *arXiv preprint arXiv:2307.08691* (2023).
- [7] Tri Dao, Daniel Y. Fu, Stefano Ermon, Atri Rudra, and Christopher Ré. 2022. FlashAttention: Fast and Memory-Efficient Exact Attention with IO-Awareness. *arXiv preprint arXiv:2205.14135* (2022).

- [8] Tri Dao, Daniel Haziza, Francisco Massa, and Grigory Sizov. 2023. Flash-decoding for long-context inference. URL: <https://pytorch.org/blog/flash-decoding/>, (Accessed: Feb. 3, 2024) (2023).
- [9] DeepSeek-AI, Daya Guo, Dejian Yang, Haowei Zhang, Junxiao Song, Ruoyu Zhang, Runxin Xu, Qihao Zhu, Shitong Ma, Peiyi Wang, Xiao Bi, Xiaokang Zhang, and et al. 2025. DeepSeek-R1: Incentivizing Reasoning Capability in LLMs via Reinforcement Learning. *arXiv preprint arXiv:2401.12948* (2025).
- [10] Bin Gao, Zhuomin He, Puru Sharma, Qingxuan Kang, Djordje Jevdjic, Junbo Deng, Xingkun Yang, Zhou Yu, and Pengfei Zuo. 2024. Cost-efficient large language model serving for multi-turn conversations with CachedAttention. In *Proceedings of the 2024 USENIX Conference on Usenix Annual Technical Conference* (Santa Clara, CA, USA) (*USENIX ATC'24*). USENIX Association, USA, Article 7, 16 pages.
- [11] Georgi Gerganov. [n.d.]. ggerganov/llama.cpp: Port of Facebook's LLaMA model in C/C++. <https://github.com/ggml-org/llama.cpp>. [Accessed 12-05-2025].
- [12] Aaron Grattafiori, Abhimanyu Dubey, Abhinav Jauhri, Abhinav Pandey, Abhishek Kadian, Ahmad Al-Dahle, Aiesha Letman, Akhil Mathur, and et al. 2024. The Llama 3 Herd of Models. *arXiv preprint arXiv:2407.21783* (2024).
- [13] Jiaao He and Jidong Zhai. 2024. FastDecode: High-Throughput GPU-Efficient LLM Serving using Heterogeneous Pipelines. *arXiv preprint arXiv:2403.11421* (2024).
- [14] Ke Hong, Guohao Dai, Jiaming Xu, Qiuli Mao, Xiuhong Li, Jun Liu, Kangdi Chen, Yuhang Dong, and Yu Wang. 2024. FlashDecoding++: Faster Large Language Model Inference on GPUs. *arXiv preprint arXiv:2311.01282* (2024).
- [15] Coleman Hooper, Sehoon Kim, Hiva Mohammadzadeh, Michael W Mahoney, Yakun Sophia Shao, Kurt Keutzer, and Amir Gholami. 2024. KVQuant: Towards 10 Million Context Length LLM Inference with KV Cache Quantization. *arXiv preprint arXiv:2401.18079* (2024).
- [16] Xuanlin Jiang, Yang Zhou, Shiyi Cao, Ion Stoica, and Minlan Yu. 2024. NEO: Saving GPU Memory Crisis with CPU Offloading for Online LLM Inference. *arXiv preprint arXiv:2411.01142* (2024).
- [17] Norm Jouppi, George Kurian, Sheng Li, Peter Ma, Rahul Nagarajan, Lifeng Nai, Nishant Patil, Suvinay Subramanian, Andy Swing, Brian Towles, Clifford Young, Xiang Zhou, Zongwei Zhou, and David A Patterson. 2023. TPU v4: An Optically Reconfigurable Supercomputer for Machine Learning with Hardware Support for Embeddings. In *Proceedings of the 50th Annual International Symposium on Computer Architecture* (Orlando, FL, USA) (*ISCA '23*). Association for Computing Machinery, New York, NY, USA, Article 82, 14 pages. <https://doi.org/10.1145/3579371.3589350>
- [18] Byeongho Kim, Sanghoon Cha, Sangsoo Park, Jieun Lee, Sukhan Lee, Shin-haeng Kang, Jinin So, Kyungsoo Kim, Jin Jung, Jong-Geon Lee, Sunjung Lee, Yoonah Paik, Hyeonsu Kim, Jin-Seong Kim, Won-Jo Lee, Yuhwan Ro, YeonGon Cho, Jin Hyun Kim, JoonHo Song, Jaehoon Yu, Seungwon Lee, Jeonghyeon Cho, and Kyomin Sohn. 2024. The Breakthrough Memory Solutions for Improved Performance on LLM Inference. *IEEE Micro* 44, 3 (May 2024), 40–48. <https://doi.org/10.1109/MM.2024.3375352>
- [19] Takeshi Kojima, Shixiang Shane Gu, Machel Reid, Yutaka Matsuo, and Yusuke Iwasawa. 2023. Large Language Models are Zero-Shot Reasoners. *arXiv preprint arXiv:2205.11916* (2023).
- [20] Woosuk Kwon, Zhuohan Li, Siyuan Zhuang, Ying Sheng, Lianmin Zheng, Cody Hao Yu, Joseph E. Gonzalez, Hao Zhang, and Ion Stoica. 2023. Efficient Memory Management for Large Language Model Serving with PagedAttention. In *Proceedings of the ACM SIGOPS 29th Symposium on Operating Systems Principles*.
- [21] Ji Lin, Jiaming Tang, Haotian Tang, Shang Yang, Wei-Ming Chen, Wei-Chen Wang, Guangxuan Xiao, Xingyu Dang, Chuang Gan, and Song Han. 2024. AWQ: Activation-aware Weight Quantization for LLM Compression and Acceleration. In *MLSys*.
- [22] Cristobal Ortega, Yann Falevoz, and Renaud Ayrignac. 2024. PIM-AI: A Novel Architecture for High-Efficiency LLM Inference. *arXiv preprint arXiv:2411.17309* (2024).
- [23] Pratyush Patel, Esha Choukse, Chaojie Zhang, Aashaka Shah, Íñigo Goiri, Saeed Maleki, and Ricardo Bianchini. 2024. Splitwise: Efficient generative LLM inference using phase splitting. *arXiv preprint arXiv:2311.18677* (2024).
- [24] Reiner Pope, Sholto Douglas, Aakanksha Chowdhery, Jacob Devlin, James Bradbury, Anselm Levskaya, Jonathan Heek, Kefan Xiao, Shivani Agrawal, and Jeff Dean. 2022. Efficiently Scaling Transformer Inference. *arXiv preprint arXiv:2211.05102* (2022).
- [25] Noam Shazeer. 2019. Fast Transformer Decoding: One Write-Head is All You Need. *arXiv preprint arXiv:1911.02150* (2019).
- [26] Ying Sheng, Lianmin Zheng, Binhang Yuan, Zhuohan Li, Max Ryabinin, Daniel Y. Fu, Zhiqiang Xie, Beidi Chen, Clark Barrett, Joseph E. Gonzalez, Percy Liang, Christopher Ré, Ion Stoica, and Ce Zhang. 2023. FlexGen: High-Throughput Generative Inference of Large Language Models with a Single GPU. *arXiv preprint arXiv:2303.06865* (2023).
- [27] Yixin Song, Zeyu Mi, Haotong Xie, and Haibo Chen. 2023. PowerInfer: Fast Large Language Model Serving with a Consumer-grade GPU. *arXiv preprint arXiv:2312.12456* (2023).
- [28] Gemma Team, Thomas Mesnard, Cassidy Hardin, Robert Dadashi, Surya Bhupatiraju, Shreya Pathak, Laurent Sifre, Morgane Rivière, Mihir Sanjay Kale, Juliette Love, and et al. 2024. Gemma: Open Models Based on Gemini Research and Technology. *arXiv preprint arXiv:2403.08295* (2024).
- [29] Hugo Touvron, Thibaut Lavril, Gautier Izacard, Xavier Martinet, Marie-Anne Lachaux, Timothée Lacroix, Baptiste Rozière, Naman Goyal, Eric Hambro, Faisal Azhar, Aurelien Rodriguez, Armand Joulin, Edouard Grave,

- and Guillaume Lample. 2023. LLaMA: Open and Efficient Foundation Language Models. *arXiv preprint arXiv:2302.13971* (2023).
- [30] Hugo Touvron, Louis Martin, Kevin Stone, Peter Albert, Amjad Almahairi, Yasmine Babaei, Nikolay Bashlykov, Soumya Batra, Prajjwal Bhargava, Shruti Bhosale, Dan Bikel, Lukas Blecher, Cristian Canton Ferrer, Moya Chen, Guillem Cucurull, David Esiobu, Jude Fernandes, Jeremy Fu, Wenyin Fu, Brian Fuller, Cynthia Gao, Vedanuj Goswami, Naman Goyal, Anthony Hartshorn, Saghar Hosseini, Rui Hou, Hakan Inan, Marcin Kardas, Viktor Kerkez, Madian Khabsa, Isabel Kloumann, Artem Korenev, Punit Singh Koura, Marie-Anne Lachaux, Thibaut Lavril, Jenya Lee, Diana Liskovich, Yinghai Lu, Yuning Mao, Xavier Martinet, Todor Mihaylov, Pushkar Mishra, Igor Molybog, Yixin Nie, Andrew Poulton, Jeremy Reizenstein, Rashi Rungta, Kalyan Saladi, Alan Schelten, Ruan Silva, Eric Michael Smith, Ranjan Subramanian, Xiaoqing Ellen Tan, Binh Tang, Ross Taylor, Adina Williams, Jian Xiang Kuan, Puxin Xu, Zheng Yan, Iliyan Zarov, Yuchen Zhang, Angela Fan, Melanie Kambadur, Sharan Narang, Aurelien Rodriguez, Robert Stojnic, Sergey Edunov, and Thomas Scialom. 2023. Llama 2: Open Foundation and Fine-Tuned Chat Models. *arXiv preprint arXiv:2307.09288* (2023).
- [31] Jason Wei, Xuezhi Wang, Dale Schuurmans, Maarten Bosma, Brian Ichter, Fei Xia, Ed Chi, Quoc Le, and Denny Zhou. 2023. Chain-of-Thought Prompting Elicits Reasoning in Large Language Models. *arXiv preprint arXiv:2201.11903* (2023).
- [32] Bingyang Wu, Shengyu Liu, Yinmin Zhong, Peng Sun, Xuanzhe Liu, and Xin Jin. 2024. LoongServe: Efficiently Serving Long-Context Large Language Models with Elastic Sequence Parallelism. In *Proceedings of the ACM SIGOPS 30th Symposium on Operating Systems Principles* (Austin, TX, USA) (*SOSP '24*). Association for Computing Machinery, New York, NY, USA, 640–654. <https://doi.org/10.1145/3694715.3695948>
- [33] Zhenliang Xue, Yixin Song, Zeyu Mi, Xinrui Zheng, Yubin Xia, and Haibo Chen. 2024. PowerInfer-2: Fast Large Language Model Inference on a Smartphone. *arXiv preprint arXiv:2406.06282* (2024).
- [34] Chengye Yu, Tianyu Wang, Zili Shao, Linjie Zhu, Xu Zhou, and Song Jiang. 2024. TwinPilots: A New Computing Paradigm for GPU-CPU Parallel LLM Inference. In *Proceedings of the 17th ACM International Systems and Storage Conference* (Virtual, Israel) (*SYSTOR '24*). Association for Computing Machinery, New York, NY, USA, 91–103. <https://doi.org/10.1145/3688351.3689164>
- [35] Chao Zeng, Songwei Liu, Yusheng Xie, Hong Liu, Xiaojian Wang, Miao Wei, Shu Yang, Fangmin Chen, and Xing Mei. 2024. ABQ-LLM: Arbitrary-Bit Quantized Inference Acceleration for Large Language Models. *arXiv preprint arXiv:2408.08554* (2024).
- [36] Susan Zhang, Stephen Roller, Naman Goyal, Mikel Artetxe, Moya Chen, Shuohui Chen, Christopher Dewan, Mona Diab, Xian Li, Xi Victoria Lin, Todor Mihaylov, Myle Ott, Sam Shleifer, Kurt Shuster, Daniel Simig, Punit Singh Koura, Anjali Sridhar, Tianlu Wang, and Luke Zettlemoyer. 2022. OPT: Open Pre-trained Transformer Language Models. *arXiv preprint arXiv:2205.01068* (2022).
- [37] Juntao Zhao, Borui Wan, Chuan Wu, Yanghua Peng, and Haibin Lin. 2024. POSTER: LLM-PQ: Serving LLM on Heterogeneous Clusters with Phase-Aware Partition and Adaptive Quantization. In *Proceedings of the 29th ACM SIGPLAN Annual Symposium on Principles and Practice of Parallel Programming* (Edinburgh, United Kingdom) (*PPoPP '24*). Association for Computing Machinery, New York, NY, USA, 460–462. <https://doi.org/10.1145/3627535.3638480>
- [38] Xuanlei Zhao, Bin Jia, Haotian Zhou, Ziming Liu, Shenggan Cheng, and Yang You. 2024. HeteGen: Heterogeneous Parallel Inference for Large Language Models on Resource-Constrained Devices. *arXiv preprint arXiv:2403.011644* (2024).
- [39] Kan Zhu, Yilong Zhao, Liangyu Zhao, Gefei Zuo, Yile Gu, Dedong Xie, Yufei Gao, Qinyu Xu, Tian Tang, Zihao Ye, Keisuke Kamahori, Chien-Yu Lin, Stephanie Wang, Arvind Krishnamurthy, and Baris Kasikci. 2024. NanoFlow: Towards Optimal Large Language Model Serving Throughput. *arXiv preprint arXiv:2408.12757* (2024).